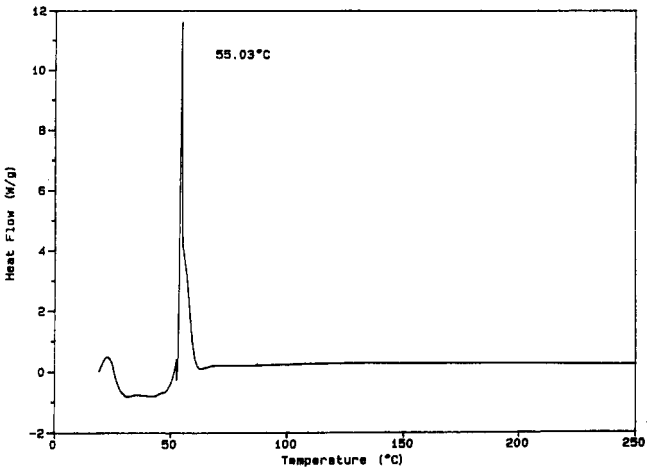

Figure 9. DSC thermogram (heating rate 15 °C/min) of an anodic surface oxide layer. The sample was scraped from a KOH-treated MCT surface (refer to text).

faces. For example, the Auger depth profiles presented in refs 2 and 3 on two different MCT samples show the peak-to-peak signal for Cd and S to be exactly opposite to the trend seen in two other more recent studies.[4,6] This discrepancy may be reconciled in light of this study, especially when it is noted that *both* CdS and S^0 contribute to the total sulfur content. Similarly, the origin of Cd lies with both MCT and CdS. Depending on the anodization time (i.e., potential) in the galvanostatic sulfidation employed in previous studies, the Cd/S ratio is likely to switch from >1 to a value <1 depending on whether S^0 formation or HgS/TeS_2 dissolution predominates. We have shown herein how the surface chemistry clearly is dependent on the sulfidization potential. At potentials lower than ~0.4 V (under the conditions pertaining to this study), the sulfidized MCT surface comprises mainly CdS; at potentials between ~0.4 and ~0.2 V, significant amounts of HgS and S^0 (along with some HgO in the case of aqueous media) are to be expected. At potentials more positive than ~0.8 V, a Cd-rich MCT surface results from the leaching of HgS and TeS_2. A puzzle not addressed in this study concerns the intriguing discrepancy between the observed and accepted value for the refractive index of CdS[4,6] and the claim[6] that two distinct forms of this material are obtained in aqueous vs nonaqueous sulfidation media. These and other issues related to the surface chemistry and electrochemistry of the passivation of MCT are being examined in this laboratory.

Acknowledgment. This research was supported, in part, by a grant from the Texas Higher Education Coordinating Board, Advanced Technology Program. We thank J. D. Luttmer of Texas Instruments, Inc., for the MCT crystals used in this study and for several discussions.

Registry No. $Hg_{0.8}Cd_{0.2}Te$, 39343-27-6; Na_2S, 1313-82-2; NaOH, 1310-73-2; CdS, 1306-23-6; HgS, 1344-48-5; HgS_2^{2-}, 26015-93-0; TeS_2, 7446-35-7; TeS_3^{2-}, 12300-21-9; S, 7704-34-9; HgO, 21908-53-2; Te, 13494-80-9; ethylene glycol, 107-21-1.

Isomorphous Substitution in $KTiOPO_4$: A Single-Crystal Diffraction Study of Members of the $K_{1-x}Na_xTiOPO_4$ Solid Solution

S. J. Crennell,† R. E. Morris,† A. K. Cheetham,† and R. H. Jarman*,‡

University of Oxford, Chemical Crystallography Laboratory, 9 Parks Rd., Oxford, OX1 3PD, U.K., and Amoco Research Center, P.O. Box 3011, Naperville, Illinois 60566

Received June 19, 1991. Revised Manuscript Received October 22, 1991

$K_{0.42}Na_{0.58}TiOPO_4$ was prepared by sodium ion exchange into $KTiOPO_4$ at 350 °C. Crystal data: orthorhombic, $Pn2_1a(33)$, a = 12.7298 (21), b = 10.6073 (13), c = 6.3074 (4) Å, V = 851.7 Å^3, Z = 4, D_c = 2.942 g cm^{-3}, $F(000)$ = 736. A sample was subsequently annealed at 700 °C. The structure of the ion-exchanged material is very similar to that found after annealing and is also consistent with that obtained in an earlier powder diffraction and solid-state NMR study of $K_{0.5}Na_{0.5}TiOPO_4$, confirming the validity of the powder work. There is considerable ordering over the two sites (site 1 0.933 (1) Na:0.067 (1) K; site 2 0.773 (7) K:0.227 (7) Na), and the single-crystal diffraction data are of sufficient resolution to detect the differing positions for the two cations on each site. Cation substitution does not affect the surrounding oxygen coordination sphere.

Introduction

The excellent nonlinear optical properties of $KTiOPO_4$ (KTP) have made it an important material for the second harmonic generation from the 1.06-μm radiation of Nd:YAG lasers.[1] Its structure[2] consists of chains in alternating TiO_6 octahedra and PO_4 tetrahedra parallel to the a and b axes, linked by helices of TiO_6 octahedra along [011] and [0$\bar{1}$1]. The octahedra in these helices are alternately cis and trans vertex sharing, building up a long–short–long chain of Ti–O bonds which is thought to be responsible for the large nonlinear coefficients of this material. The cations sit in channels running parallel to [100] and [001] with distorted hexagonal rings of oxygen atoms defining the windows between sites. All of the atoms in the structure are on general positions, making the structure very versatile with respect to isomorphous substitution:

† University of Oxford.
‡ Amoco Research Center.

(1) Bierlein, J. D.; Arweiler, C. B. *Appl. Phys. Lett.* **1986**, *49*, 917.
(2) Tordjman, I.; Masse, R.; Guitel, J. C. *Z. Kristallogr.* **1974**, *134*, 103.

0897-4756/92/2804-0082$03.00/0

K has been replaced by Na, Rb, Tl, Cs, and NH_4; Ti by Ge, Sn, Zr and by atoms of different valence such as Ga and Nb; P by As and Si.[3] A more complete review is available in ref 4. Solid solutions exist between many of these species, allowing the possibility of selective modification of the nonlinear optical properties.[5] There are two formula units per asymmetric unit, and it has been shown[6-8] that substitution for K and Ti occurs preferentially at one of the two sites, depending, in the case of K, on the size of the substituting species. Ion exchange takes place readily in molten salts of the alkali metals and is used in the fabrication of KTP wave guides of potential commercial importance.[9] The question arises as to whether the ordered cation distributions that are observed in high-temperature preparations are also present in waveguide crystals that have been ion-exchanged at lower temperatures. We report single-crystal X-ray diffraction studies in the $K_{1-x}Na_xTiOPO_4$ solid solution, comparing the cation distribution of an ion-exchanged material with that of a sample that has been annealed at high temperatures.

Experimental Section

$KTiOPO_4$ (KTP) crystals were grown from the flux of composition: 53% KTP, 47% ($07.K_2O{:}0.3P_2O_5$) suggested by Iliev et al.[10] The starting materials (K_2CO_3, $NH_4H_2PO_4$, and TiO_2) were melted into a platinum crucible and held at 1000 °C for 24 h to allow the system to reach equilibrium and then cooled at 3 °C/h to 700 °C. Transparent colorless crystals were extracted from the flux by prolonged boiling in deionized water. A powder X-ray diffraction pattern indicated that the crystals were pure KTP.

Previous work on ion exchange in KTP powders[11] had shown that to obtain 50% potassium substitution by sodium, a $NaNO_3$:KTP molar ratio of 10:1 was required. Powders of this composition were left at 350 °C for varied periods of time, and analytical electron microscopy[12] carried out on the $K_{1-x}Na_xTiOPO_4$ products indicated that the material was homogeneous after 2 weeks under the ion-exchange conditions. A 2-g sample of KTP crystals was mixed with a 10:1 molar excess of $NaNO_3$ powder and heated at 350 °C for 2 weeks, after which the crystals were readily removed by boiling in deionized water. The crystals appeared white and opaque but with sharp crystal form. Finally a sample of the crystals was heated to 700 °C for 3 days to bring the system to thermodynamic equilibrium.

A typical specimen of the ion-exchanged $K_{1-x}Na_xTiOPO_4$ crystals was glued to a glass fiber and mounted on an Enraf-Nonius CAD4 diffractometer. Reflection positions at high χ and θ were measured from a rotation photograph and centered to give the unit cell: a = 12.730 (2), b = 10.607 (1), c = 6.3074 (4) Å. Data, containing all Friedel pairs, were collected out to 54° in θ. Details of the data collection are given in Table I. An annealed crystal of size 0.13 × 0.22 × 0.30 mm was similarly mounted on the diffractometer. An automatic interrupted search routine produced 25 reflections which were centered to determine the unit cell.

Table I. Data Collection Parameters for the $K_{1-x}Na_xTiOPO_4$ Crystals

	Ion-exchanged	Ion-exchanged and annealed
mol formula	$K_{.42}Na_{0.58}TiOPO_4$	$K_{.43}Na_{0.57}TiOPO_4$
formula wt	188.68g	188.79
cryst size, mm	0.13 × 0.15 × 0.32	0.13 × 0.22 × 0.30
cryst syst	orthorhombic	orthorhombic
a/Å	12.7298 (21)	12.7378 (9)
b/Å	10.6073 (13)	10.6081 (15)
c/Å	6.3074 (4)	6.3077 (5)
V/Å^3	851.7	852.3
space group	Pn 2_1a (33)	Pn2_1a (33)
D_c/g cm^{-3}	2.942	2.960
F(000)	736	736
Z	8	8
linear abs coeff	27.356	28.0512
X-radiation	Mo Kα graphite monochromator	
2θ max/deg	108	110
scan type	ω-2θ	ω-2θ
scan width/deg	0.83 + 0.35 tan θ	0.92 + 0.35 tan θ
min/max scan	1.5, 6.7	1.8, 6.7
total data	10265	11037
observed data	8094	8180
$I > n\sigma(I)$, n =	3	3
abs. corr min, max	1.16, 1.38	1.00, 1.37
min h, k, l	0, 0, 0	0, 0, 0
max h, k, l	29, 24, 14	29, 24, 14
no. of params	157	157
weighting scheme coeffs	9.8 (2), −1.3 (1), 7.9 (2)	$w[1 - \Delta F/6\sigma F^2]^2$ 6.56, −1.80, 5.11
$\Delta\rho$/e Å^{-3}	2.00	1.78
final shift/error	0.08	0.002
final $R = \sum\Delta/\Delta F_o$, %	4.53	3.08
$R_w = (\sum w\Delta F^2/\sum wF_o^2)^{1/2}$ %	5.54	3.70

Later, higher angle reflections (θ range 34.5–40°) were centered to give the cell: a = 12.7378 (9), b = 10.6081 (14), c = 6.3077 (5) Å. Data were collected out to 55° in θ, collecting all Friedel pairs, with three standard reflections, monitored for intensity variation every hour, showing no systematic trends. Details of the data collection are given in Table I. Data reduction and all subsequent calculations were carried out using the Oxford package CRYSTALS,[13] with data from ψ scans on two reflections used to obtain a semiempirical absorption correction. Complex scattering factors were taken from the International Tables for Crystallography.[14]

The Ti and P positions from the $K_{1/2}Na_{1/2}TiOPO_4$ structure obtained from Rietveld analysis of combined neutron time-of-flight and X-ray powder diffraction data[6] were used as a starting model for the annealed system. The K position was readily apparent from a difference Fourier map, and after least-squares refinement of the positional parameters of these five atoms, the oxygens were found in a subsequent difference Fourier map. The sodium site was distinguished from that of the oxygen atoms using bond length criteria. The cation ordering was apparent from the marked difference in scattering from the two sites. The final full matrix least-squares refinement included anisotropic thermal parameters and converged to an R factor of 3.71%, but with peaks in an difference Fourier map of ρ = 5.35 and 2.15 e/Å^3 close to K(2) and Na(1), respectively. These were thought to be the positions of small amounts of K in the Na(1) cavity and Na in the K(2) cavity and were refined isotropically as such with the other atoms to give a final R = 3.08% and a final difference Fourier with a maximum peak of ρ = 1.8 e/Å^3. The cation occupancy was restrained so that the total occupancy of each framework cavity was equal to 1. The only high correlations were between the atomic y parameters, the direction along which the origin is not fixed by symmetry but is fixed in CRYSTALS as the center of mass of the atomic y coordinates.

This structure was taken as the starting model for the analysis of the unannealed ion-exchanged crystal. The minor cation

(3) Crosnier, M. P.; Guyomard, D.; Verbaere, A.; Piffard, Y. *Eur. J. Solid State Inorg. Chem.* **1990**, *27*, 845.
(4) Stucky, G. D.; Phillips, M. L. F.; Gier, T. E. *Chem. Mater.* **1989**, *1*, 492.
(5) Phillips, M. L. F.; Gier, T. E.; Eddy, M. M.; Keder, N. L.; Stucky, G. D.; Bierlein, J. D. *Solid State Ionics* **1989**, *32/33*, 147.
(6) Crennell, S. J.; Owen, J. J.; Grey, C. P.; Cheetham, A. K.; Kaduk, J. A.; Jarman, R. H. *J. Mater. Chem.* **1991**, *1*, 113.
(7) Crennell, S. J.; Cheetham, A. K.; Kaduk, J. A.; Jarman, R. H. *J. Mater. Chem.* **1991**, *1*, 297.
(8) Crennell, S. J.; Owen, J. J.; Cheetham, A. K.; Kaduk, J. A.; Jarman, R. H. *Eur. J. Solid State Inorg. Chem.* **1991**, *28*, 397.
(9) Bierlein, J. D.; Laubacher, D. B.; Brown, J. B.; van der Poel, C. J. *Appl. Phys. Lett.* **1990**, *56*, 1725.
(10) Iliev, K.; Peshev, P.; Nikolov, V.; Koseva, I. *J. Cryst. Growth.* **1990**, *100*, 225.
(11) Jarman, R. H. *Solid State Ionics* **1989**, *32/33*, 45.
(12) Cheetham, A. K.; Skarnulis, A. J. *Anal. Chem.* **1981**, *53*, 1060.
(13) Watkin, D. J.; Carruthers, J. K.; Betteridge, P. W. (1985) CRYSTALS *user guide*; Chemical Crystallography Laboratory: University of Oxford, Oxford, U.K.
(14) *International Tables for X-ray Crystallography*; Kynoch Press: Birmingham, U.K., 1974; Vol. IV.

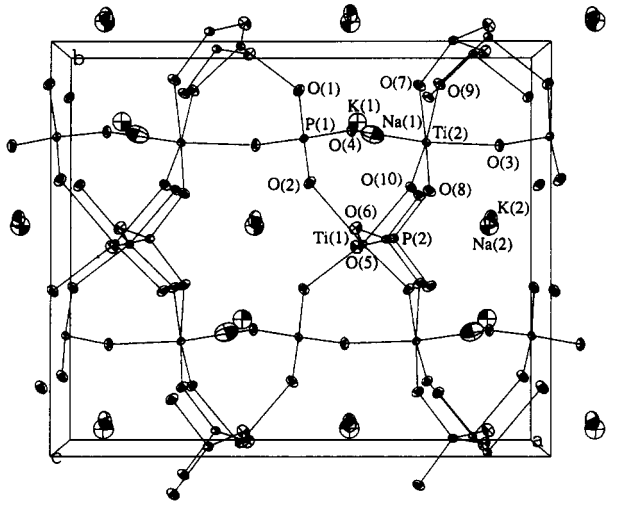

Figure 1. Projection of the unit cell of $K_{0.5}Na_{0.5}TiOPO_4$ along [001].

positions were individually identified and refined with isotropic temperature factors. The other atoms refined with anisotropic thermal parameters to give a final $R = 4.53\%$. A difference Fourier contained no significant residual peaks, the maximum being 1.8 e/Å^3. Final atom coordinates and thermal parameters for both refinements are given in Table II, bond lengths and angles are in Table III and a view of the unit cell is shown in Figure 1.

Discussion

The $K_{1-x}Na_xTiOPO_4$ solid solution series is isomorphous with KTP. The unit cell volumes of these specimens, 852.3 (0.3) and 851.7 (0.2)Å^3, indicate compositions of $K_{0.47}Na_{0.53}TiOPO_4$ and $K_{0.46}Na_{0.54}TiOPO_4$, respectively, from a plot of cell volume against composition in this solid solution,[11] in reasonable agreement with those obtained by refinement of the occupancies. Rather surprisingly, remarkable consistency is found between the distribution observed for the ion-exchanged crystal and that of the high-temperature crystal. There is considerable ordering of K and Na over the two cation sites, with the majority of the sodium in site 1 and the potassium in site 2, as observed in an earlier powder diffraction study.[6] The validity of the ordering determined by powder diffraction and solid-state NMR is, therefore, confirmed. However, the single-crystal structure is of sufficiently high resolution that the position of the minor cation in each site can be determined independently, and its atomic coordinates and isotropic thermal parameters refined. The oxygen coordination around the cation sites is shown in Figures 2 and 3. The fact that the structure of the ion-exchanged KNaTP crystal is well defined, together with the existence of diffraction data out to 54°, implies that there are no significant concentration gradients remaining in the ion-exchanged crystal. Annealing the sample marginally improves the precision of the atomic coordinates and bond lengths but does not materially alter the structure.

The substitution of the different size cations does not seem to affect the cavity in which they lie, since the anisotropic temperature factors of oxygen are comparable with those of KTP and $KSnOPO_4$ in a similar X-ray single-crystal study.[15] Bond valence calculations[16] carried out on the cation–oxygen distances of all four cations (Table IV) show that the bond valences of the major

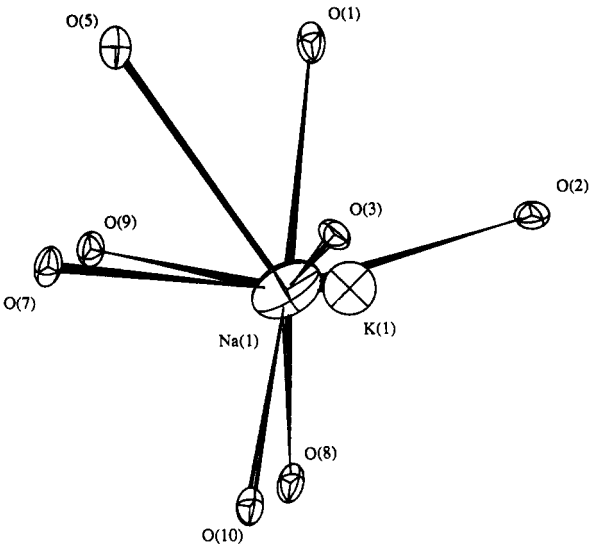

Figure 2. Oxygen coordination around the K(1) site which is mainly occupied by sodium. The position of the potassium ion is also shown, refined with isotropic temperature factors.

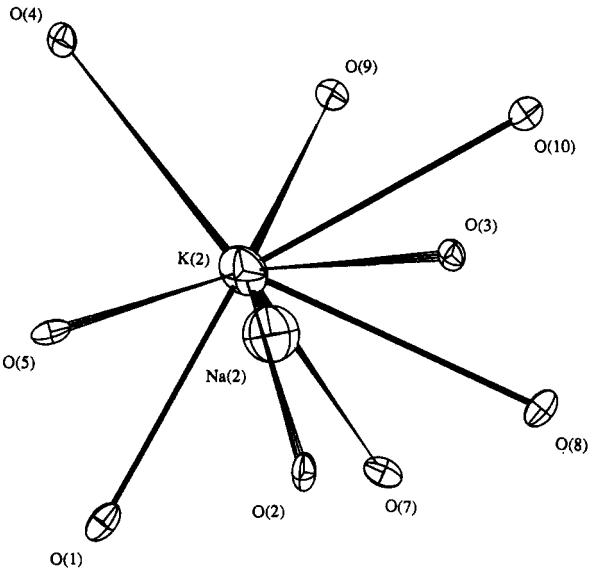

Figure 3. Oxygen coordination around the potassium ion in the K(2) site. The position of the minor Na(2) site is also shown.

cations (Na(1) and K(2)) are very similar to those of the parent species. The minor K(1) site has a larger bond valence than in KTP, but the occupancy of this site is rather low for accurate determination. Although the minor cation Na(2) in NKaTP has a very similar bond valence to that in the β-NaTP solid solution end member, the coordination is subtly different, reflecting slight changes in the relative positions of the cation and framework oxygen atoms.

It has been reported that the NLO coefficient of KNaTP is essentially unchanged from that of KTP but that of β-NaTP is an order of magnitude inferior.[17] These data were obtained from powder SHG tests and hence must be treated with some caution, given the number of variables involved in the measurement. Nevertheless, our own measurements from powder SHG tests are in qualitative agreement with those in ref. 17. It is instructive to compare the structure of the mixed phase with those of the end-members in the context of the nonlinear optical

(15) Thomas, P. A.; Glazer, A. M.; Watts, B. E. *Acta Crystallogr.* **1990**, *B46*, 333.

(16) Brown, I. D. *Structure and Bonding in Crystals*; O'Keefe, M., Navrotsky, A., Eds.; Academic Press: New York, 1980; Vol. II, pp 1–30.

(17) Phillips, M. L. F.; Harrison, W. T. A.; Gier, T. E.; Stucky, G. D. *Proc SPIE–Int. Soc. Opt. Eng.* **1989**, *1104*, 225.

Table II. Atomic Coordinates for $K_{1-x}Na_xTiOPO_4$[a]

1. Ion-Exchanged Crystal

atom	x/a	y/b	z/c	occupancy	U(equiv) or U(iso)/Å²
Ti(1)	0.37293 (2)	0.0108 (1)	0.49432 (3)		0.0051
Ti(2)	0.24501 (1)	0.2629 (1)	0.26564 (3)		0.0052
P(1)	0.49518 (3)	0.2751 (1)	0.33889 (6)		0.0055
P(2)	0.18385 (3)	0.5243 (1)	0.49875 (6)		0.0054
K(1)	0.381 (1)	0.327 (1)	0.786 (2)	0.0669 (13)	0.026 (3)
Na(1)	0.3488 (2)	0.2950 (2)	0.7686 (2)	0.9332 (13)	0.0271
K(2)	0.09840 (5)	0.0747 (1)	0.6793 (1)	0.773 (7)	0.0197
Na(2)	0.0989 (6)	0.0581 (7)	0.773 (1)	0.227 (7)	0.028 (1)
O(1)	0.4822 (1)	0.1664 (1)	0.4931 (2)		0.0096
O(2)	0.50553 (9)	0.3985 (1)	0.4683 (2)		0.0094
O(3)	0.39902 (8)	0.2914 (1)	0.1922 (2)		0.0080
O(4)	0.59272 (7)	0.2559 (1)	0.1978 (2)		0.0088
O(5)	0.1157 (1)	0.5526 (1)	0.3047 (2)		0.0087
O(6)	0.11130 (9)	0.5033 (1)	0.6870 (2)		0.0087
O(7)	0.2553 (1)	0.6393 (1)	0.5316 (2)		0.0088
O(8)	0.2552 (1)	0.4093 (1)	0.4642 (2)		0.0089
O(9)	0.22728 (9)	0.6545 (1)	−0.0347 (2)		0.0080
O(10)	0.2240 (1)	0.3986 (1)	0.0275 (2)		0.0084

	U(11)	U(22)	U(33)	U(23)	U(13)	U(12)
Ti(1)	0.00609 (5)	0.00461 (5)	0.00488 (5)	0.00061 (5)	−0.00014 (4)	−0.00039 (5)
Ti(2)	0.00534 (5)	0.00436 (5)	0.00604 (5)	−0.00025 (5)	−0.00042 (4)	0.00070 (5)
P(1)	0.00462 (9)	0.0051 (1)	0.0072 (1)	0.00046 (8)	−0.00013 (7)	−0.00079 (7)
P(2)	0.0074 (1)	0.0047 (1)	0.00471 (9)	−0.00066 (7)	−0.00009 (8)	0.00019 (7)
Na(1)	0.041 (1)	0.0247 (7)	0.0208 (5)	−0.0011 (5)	−0.0029 (6)	−0.0066 (7)
K(2)	0.0136 (2)	0.0253 (3)	0.0253 (3)	0.0020 (2)	−0.0064 (2)	0.0011 (2)
O(1)	0.0103 (3)	0.0103 (3)	0.0120 (4)	0.0051 (3)	0.0025 (3)	0.0036 (3)
O(2)	0.0085 (3)	0.0088 (3)	0.0139 (4)	0.0041 (3)	−0.0008 (3)	−0.0024 (2)
O(3)	0.0054 (3)	0.0104 (3)	0.0094 (3)	0.0016 (3)	−0.0008 (2)	0.0001 (2)
O(4)	0.0057 (2)	0.0115 (3)	0.0107 (3)	−0.0014 (3)	0.0008 (2)	−0.0001 (2)
O(5)	0.0117 (3)	0.0119 (4)	0.0051 (3)	0.0002 (2)	0.0008 (2)	0.0027 (3)
O(6)	0.0109 (3)	0.0113 (3)	0.0056 (2)	0.0001 (3)	−0.0006 (2)	0.0022 (3)
O(7)	0.0108 (3)	0.0078 (3)	0.0108 (3)	−0.0037 (3)	−0.0028 (3)	0.0026 (2)
O(8)	0.0117 (3)	0.0076 (3)	0.0105 (3)	0.0032 (3)	0.0028 (3)	0.0033 (2)
O(9)	0.0089 (3)	0.0073 (3)	0.0091 (3)	−0.0023 (2)	−0.0001 (3)	0.0022 (2)
O(10)	0.0092 (3)	0.0081 (3)	0.0096 (3)	0.0017 (2)	0.0002 (3)	0.0030 (2)

2. Annealed Crystal

atom	x/a	y/b	z/c	occupancy	U(equiv) or U(iso)/Å²
Ti(1)	0.37298 (1)	0.99779 (8)	0.49372 (2)		0.0049
Ti(2)	0.24527 (1)	0.25018 (8)	0.26508 (2)		0.0050
P(1)	0.49540 (2)	0.26205 (8)	0.33875 (5)		0.0053
P(2)	0.18392 (2)	0.51134 (8)	0.49832 (5)		0.0053
K(1)	0.3801 (8)	0.319 (1)	0.783 (2)	0.056 (6)	0.0023 (2)
Na(1)	0.3489 (1)	0.2819 (1)	0.7677 (2)	0.944 (6)	0.0268
K(2)	0.09819 (4)	0.06176 (9)	0.6785 (1)	0.810 (4)	0.0196
Na(2)	0.1000 (5)	0.0431 (6)	0.778 (1)	0.190 (4)	0.0030 (1)
O(1)	0.48213 (8)	0.1532 (1)	0.4928 (2)		0.0092
O(2)	0.50561 (7)	0.3856 (1)	0.4690 (2)		0.0089
O(3)	0.39919 (6)	0.2786 (1)	0.1917 (1)		0.0079
O(4)	0.59293 (6)	0.2430 (1)	0.1979 (1)		0.0082
O(5)	0.11605 (8)	0.5398 (1)	0.3035 (1)		0.0084
O(6)	0.11112 (7)	0.4902 (1)	0.6867 (1)		0.0088
O(7)	0.25635 (8)	0.6265 (1)	0.5312 (2)		0.0086
O(8)	0.25533 (7)	0.3966 (1)	0.4640 (2)		0.0085
O(9)	0.22710 (7)	0.6417 (1)	0.9645 (1)		0.0079
O(10)	0.22419 (7)	0.3858 (1)	0.0270 (2)		0.0089

	U(11)	U(22)	U(33)	U(23)	U(13)	U(12)
Ti(1)	0.00547 (4)	0.00451 (4)	0.00487 (4)	0.00062 (4)	−0.00016 (4)	−0.00042 (4)
Ti(2)	0.00474 (4)	0.00427 (4)	0.00619 (4)	−0.00022 (4)	−0.00032 (3)	0.00063 (4)
P(1)	0.00409 (6)	0.00520 (8)	0.00727 (8)	0.00048 (7)	−0.00028 (6)	−0.00092 (6)
P(2)	0.00700 (7)	0.00468 (8)	0.00481 (7)	−0.00075 (6)	−0.00017 (7)	0.00033 (6)
Na(1)	0.0440 (8)	0.0232 (5)	0.0199 (4)	−0.0008 (3)	−0.0036 (4)	−0.0061 (5)
K(2)	0.0135 (1)	0.0259 (2)	0.0256 (2)	−0.0020 (2)	−0.0069 (1)	0.0013 (1)
O(1)	0.0098 (3)	0.0104 (3)	0.0118 (3)	0.0053 (2)	0.0030 (2)	0.0038 (2)
O(2)	0.0080 (2)	0.0081 (2)	0.0139 (3)	0.0042 (2)	−0.0010 (2)	−0.0022 (2)
O(3)	0.0052 (2)	0.0101 (2)	0.0098 (3)	0.0011 (2)	−0.0011 (2)	−0.0005 (2)
O(4)	0.0046 (2)	0.0120 (3)	0.0105 (3)	−0.0011 (2)	0.0013 (2)	−0.0000 (2)
O(5)	0.0115 (3)	0.0114 (3)	0.0051 (2)	−0.0002 (2)	0.0014 (2)	0.0033 (2)
O(6)	0.0112 (2)	0.0114 (3)	0.0056 (2)	0.0002 (2)	−0.0009 (2)	0.0022 (2)
O(7)	0.0114 (3)	0.0076 (2)	0.0100 (3)	−0.0035 (2)	−0.0024 (2)	0.0032 (2)
O(8)	0.0109 (3)	0.0071 (2)	0.0109 (3)	0.0034 (2)	0.0030 (2)	0.0031 (2)
O(9)	0.0085 (2)	0.0074 (2)	0.0090 (2)	−0.0020 (2)	0.0001 (2)	0.0019 (2)
O(10)	0.0096 (2)	0.0079 (2)	0.0102 (3)	0.0014 (2)	−0.0001 (2)	0.0028 (2)

[a] U(equiv) values esds are quoted when the anisotropic thermal parameters have been calculated for the atom in question. U(equiv) is defined as the radius of a sphere of volume equal to that of the thermal ellipsoid, the cube root of the product of the three principal ellipsoid axes. U(iso) values are quoted when the scattering was too low to allow anisotropic thermal parameters to be realistically calculated.

Table III. Bond Distances and Angles, Comparing the Two Ion-Exchanged Samples with the Earlier Powder Diffraction Results

	ion-exchanged	annealed	powder[6]		ion-exchanged	annealed	powder[6]
Ti(1)–O(1)	2.159 (1)	2.1563 (9)	2.129 (5)	Ti(2)–O(3)	2.037 (1)	2.0366 (8)	2.001 (6)
–O(2)	1.967 (1)	1.9656 (9)	1.979 (5)	–O(4)	1.954 (1)	1.9556 (7)	1.988 (6)
–O(5)	2.013 (1)	2.0096 (9)	2.016 (5)	–O(7)	1.974 (1)	1.9748 (9)	1.907 (6)
–O(6)	1.951 (1)	1.9494 (8)	1.942 (6)	–O(8)	2.000 (1)	2.0007 (9)	2.055 (6)
–O(9)	1.996 (1)	1.9969 (8)	1.951 (6)	–O(9)	1.741 (1)	1.7417 (9)	1.796 (6)
–O(10)	1.727 (1)	1.7283 (9)	1.744 (5)	–O(10)	2.097 (1)	2.0971 (9)	2.038 (6)
P(1)–O(1)	1.517 (1)	1.5188 (9)	1.550 (3)	P(2)–O(5)	1.529 (1)	1.5323 (9)	1.531 (3)
–O(2)	1.548 (1)	1.5520 (9)	1.554 (3)	–O(6)	1.521 (1)	1.5237 (9)	1.532 (3)
–O(3)	1.544 (1)	1.5470 (9)	1.546 (3)	–O(7)	1.545 (1)	1.5444 (9)	1.537 (3)
–O(4)	1.541 (1)	1.5404 (9)	1.543 (3)	–O(8)	1.536 (1)	1.5349 (9)	1.554 (3)
K(1)–O(1)	2.82 (1)	2.85 (1)		Na(1)–O(1)	2.787 (2)	2.784 (2)	2.797 (5)
–O(2)	2.66 (1)	2.64 (1)		–O(3)	2.748 (2)	2.750 (2)	2.729 (5)
–O(3)	2.60 (1)	2.62 (1)		–O(5)	2.620 (2)	2.617 (2)	2.709 (5)
–O(5)	2.91 (2)	2.96 (1)		–O(7)	2.698 (3)	2.698 (2)	2.752 (5)
–O(7)	3.07 (1)	3.10 (1)		–O(8)	2.564 (2)	2.564 (2)	2.571 (5)
–O(8)	2.73 (1)	2.70 (1)		–O(9)	2.612 (3)	2.609 (2)	2.684 (6)
–O(9)	3.05 (2)	3.07 (1)		–O(10)	2.529 (2)	2.532 (2)	2.537 (6)
–O(10)	2.63 (1)	2.609 (9)					
K(1)–Na(1)	0.54 (1)	0.57 (1)					
K(2)–O(1)	2.721 (1)	2.725 (1)	2.741 (6)	Na(2)–O(1)	2.387 (7)	2.389 (8)	
–O(2)	2.927 (2)	2.933 (1)	2.992 (5)	–O(2)	2.459 (7)	2.481 (8)	
–O(3)	3.006 (1)	3.005 (1)	3.082 (6)	–O(5)	2.799 (6)	2.776 (7)	
–O(4)	3.059 (1)	3.056 (1)	3.010 (5)	–O(7)	2.583 (6)	2.607 (7)	
–O(5)	2.738 (1)	2.741 (1)	2.829 (6)	–O(8)	2.680 (7)	2.720 (8)	
–O(7)	2.969 (1)	2.975 (1)	2.928 (6)				
–O(8)	3.127 (2)	3.129 (1)	3.114 (6)				
–O(9)	2.732 (1)	2.737 (1)	2.685 (7)				
O(10)	3.085 (1)	3.085 (1)	3.083 (6)				
K(2)–Na(2)	0.615 (8)	0.661 (7)					

Table IV. Bond Valence Parameters of $K_{1-x}Na_xTiOPO_4$ and the Solid Solution End Members

structure	site 1	site 2	ref
ion-exchanged sample			this work
Na	0.77	0.74	
K	1.45	1.14	
annealed sample			this work
Na	0.77	0.76	
K	1.44	1.13	
β-$NaTiOPO_4$	0.79	0.73	23[a]
$KTiOPO_4$	1.22	1.11	2
$K_{0.5}Na_{0.5}TiOPO_4$			6
Na	0.76	0.52	
K	1.75	0.99	

[a] The bond valence parameters calculated for β-$NaTiOPO_4$ have been calculated from the atom coordinates given in ref 23. Previously[6] the β-$NaTiOPO_4$ bond valence parameters were calculated using the Na–O bond distances presented in ref 16, where the shortest Na–O distance was omitted, having a severe effect on the Na(2) site bond valence.

properties of the series. Selected crystallographic data are shown in Table V. We focus primarily on the coordination spheres of the two oxygen atoms, O(9) and O(10), which are involved in the long–short bond alternation in the Ti–O chains. First we note that the bond lengths in the Ti–O chains vary negligibly across the series, which, given the apparent success of the previous model in describing the NLO properties of KTP by consideration of contributions from individual bonds,[18,19] is somewhat surprising. Indeed, in view of the correlation observed between the bond lengths in the Ti–O chain and NLO properties of the NH_4–H isomorph series of KTP,[22] we might have expected to observe a lengthening of at least one of the short Ti–O bonds in β-NaTP. Ti(1)–O(9) shows the most variation with Na substitution, but even this is less than 1%. The four phosphate Ti–O bonds in each octahedron also remain essentially unchanged, with the exception of Ti(1)–O(1) (the long bond trans to Ti(1)–O(10)), which lengthens by 3% in β-NaTP compared with KTP.[17] This apparent rigidity of the $TiOPO_4$ framework when subjected to ion exchange suggests that cation coordination is playing an important role in determining the NLO properties of the materials.

Any model of the NLO coefficient which merely considers either the magnitude of individual bond lengths or the dispersion of the bond lengths[15,18,19] would appear to be inadequate on the basis of the results for the KTP–β-NaTP system as has been noted previously in a discussion of the arsenate analogue KTA.[4] We have assumed that the bulk NLO coefficient is directly proportional to the microscopic second-order susceptibility of the TiO_6 fragments. Strictly speaking, it is necessary to consider the relative orientation of all the fragments in the unit cell, but we expect that the small angular variations observed (see later) are not sufficient to explain the large changes in the NLO coefficient. Obviously, the NLO properties will be determined by the electronic structure of the material, which will in turn be influenced by cation substitution. The NLO coefficient appears to be sensitive to perturbations in the electronic structure more subtle than any that manifest themselves in modifications to the $TiOPO_4$ framework, as registered in individual bond lengths. We compare a number of salient features of the three compositions in Tables V and VI. In the search for a particular structural parameter that correlates with the trend in NLO properties, we would expect to see very little variation of that parameter between KTP and KNaTP, but presumably a significant change between the latter

(18) Zumsteg, F. C.; Bierlein, J. D.; Gier, T. E. *J. Appl. Phys.* **1976**, *47*, 4980.
(19) Hansen, N. K.; Protas, J.; Marnier, G. *C.R. Acad. Sci. Paris, Ser. II* **1988**, *307*, 475.
(20) Jarman,. R. H.; Grubb, S. G., *Proc. SPIE Conference Ceram. Inorg. Cryst. Opt. Electroopt. Conv.* **1988**, *968*, 108.
(21) Munowitz, M.; Jarman, R. H.; Harrison, J. F. *J. Phys. Chem.*, in press.
(22) Eddy, M. M.; Gier, T. E.; Keder, N. L.; Stucky, G. D.; Cox, D. E.; Bierlein, J. D.; Jones, G. *Inorg. Chem.* **1988**, *27*, 2158.

Table V. Selected Bond Distances and Angles in the Ion-Exchanged KNTP and the Solid Solution End Members

	KTP[2]	KNTP (ion exchanged)	β-NTP[23]
Ti(1)–O(1)	2.161 (4)	2.159 (1)	2.226 (6)
–O(2)	1.957 (4)	1.967 (1)	1.978 (6)
–O(5)	2.047 (4)	2.013 (1)	2.000 (6)
–O(6)	1.900 (4)	1.951 (1)	1.937 (5)
–O(9)	1.993 (4)	1.996 (1)	2.005 (6)
–O(10)	1.718 (4)	1.727 (1)	1.717 (6)
Ti(2)–O(3)	2.037 (3)	2.037 (3)	2.019 (5)
–O(4)	1.979 (3)	1.954 (1)	1.924 (5)
–O(7)	1.966 (4)	1.974 (1)	1.991 (6)
–O(8)	1.994 (4)	2.000 (1)	1.999 (6)
–O(9)	1.738 (4)	1.741 (1)	1.758 (6)
–O(10)	2.101 (4)	2.097 (1)	2.099 (6)
K(1)–O(9)	2.987 (4)	2.612 (3)	2.745 (8)
–O(10)	2.717 (4)	2.529 (2)	2.525 (7)
K(2)–O(9)	2.765 (4)	2.732 (1)	2.644 (8)
–O(10)	3.055 (4)	3.085 (1)	
O(9)–Ti(1)–O(10)	94.8 (2)	94.62 (5)	95.0 (3)
O(9)–Ti(2)–O(10)	174.7	175.43 (6)	175.2 (3)
Ti(1)–O(9)–Ti(2)	135.5	134.43 (7)	130.8 (3)
Ti(1)–O(10)–Ti(2)	132.9	130.58 (7)	132.3 (3)

Table VI. Bond Valences of the O(9) and O(10) TiO_6 Helices in KNTP with KTP and β-NTP for Comparison

	KTP[2]	ion-exchanged KNTP	β-NTP[23]
		O(9)	
Ti(1)	0.619	0.613	0.59
Ti(2)	1.23	1.22	1.17
K(1)	0.099	0.113 (Na)	0.078 (Na)
K(2)	0.181	0.197	0.103 (Na)
P(1)	0.013	0.014	0.010
P(2)	0.010	0.011	0.010
total	2.16	2.17	1.97
		O(10)	
Ti(1)	1.30	1.27	1.30
Ti(2)	0.46	0.466	0.46
K(1)	0.206	0.137 (Na)	0.142 (Na)
K(2)	0.083	0.076	0.014 (Na)
P(1)	0.011	0.010	0.015
P(2)	0.011	0.011	0.010
total	2.08	1.97	1.95

composition and β-NaTP. Two structural parameters that satisfy this condition are the Ti(1)–O(9)–Ti(2) bond angle and the bond valence sum for O(9). The Ti(1)–O(9)–Ti(2) angle in KNaTP is 134.4°, compared with 135.5 and 130.8° for KTP and β-NaTP, respectively. By contrast, Ti(1)–O(10)–Ti(2) shows very little variation with cation type. In KTP and KNaTP, O(9) and O(10) are each bound to two cations, whereas O(10) is bound to Na(1) in β-NaTP. In both cases, the bond valence sums decrease by about 0.1 when K is replaced by Na, but, significantly perhaps in the case of O(9), all of the decrease occurs between KNaTP and β-NaTP. By way of comparison, the eight phosphate oxygens show the following: the bond valence sums of O(2), O(3), and O(8) decrease, while the remaining oxygens show essentially no change and the coordination numbers of O(2), O(3), O(4), and O(8) are reduced by one, reflecting the lower coordination numbers of Na(1) and Na(2) compared with K(1) and K(2).

According to an elementary orbital picture for the bonding in a TiO_6 octahedron, sigma bonds between Ti and six oxygen atoms are derived from the 4p, 4s and the $3d_{z^2}$ and $3d_{x^2-y^2}$ atomic orbitals of Ti and six sp hybrids from O. This leaves any electrons on oxygen not involved in bonds to P and K (or Na) and the t_{2g} set of Ti 3d atomic orbitals available for π-bonding. It has been proposed that the ferroelectric distortion of the TiO_6 octahedron in KTP is stabilized through this mechanism.[20] Both the nonbonded orbitals on O and π bonds constitute the highest occupied "molecular" orbitals (HOMOs) in the valence band of KTP. The HOMOs are expected to make significant contributions to the hyperpolarizability, particularly where transitions involve a large change in dipole moment. We therefore expect the Ti–O π bonds to play a role similar to that of the π systems of aromatic molecules. We should also note that, on the basis of the results of ab initio electronic structure calculations on TiO_6 octahedra,[21] the contributions of Ti–O σ bonds may also be substantial. The presence of continuous Ti–O chains is also perhaps significant, affording the possibility of delocalization, with the result being a collective response of electrons to applied optical fields; nevertheless, we would not expect extensive delocalization, given the long–short Ti–O bond alternation. The apparent strong correlation between the NLO response and the Ti(1)–O(9)–Ti(2) angle may indeed be due to the sensitivity of the degree of delocalization to the magnitude of this angle, the role of the cation being to modify this angle through its interactions with O(9). We note with interest that calculations based solely on a consideration of individual bonds or octahedra underestimate the value of the NLO coefficient.[18,19] As has been noted previously,[4] other isomorphs also follow this trend, including NH_4HTP (127°),[22] AgTP (129°),[4] and NaTA (135°).[23] NH_4HTP also shows an increase in one of the short Ti–O bonds, as mentioned earlier.

An alternative approach is to consider the effect of cation basicity on the electronic structure. It has been proposed[17] that the basicity of the monovalent cation affects the Ti–O bonding through its interaction with the O atoms in the framework; the argument being that in the case of β-NaTP, the short Na–O(9) distance (compared with K–O(9)) causes an alteration of the Ti–O(9) bond polarizability through a weakening of the latter's "bond valence". According to chemical convention, we understand the relationship between bond length and valence to be invariant (we have used this concept to compute individual bond valences from the crystallographic data), and hence we would expect no significant changes in the Ti–O bond valences across the KTP–β-NaTP series. This model has recently been refined and improved by consideration of a molecular orbital picture of an O–Ti–O linkage.[23,24] It has been proposed[23,24] that reduced ionicity of the framework lowers the contribution of orbitals located on the framework to the numerator in the perturbative expression for the hyperpolarizability

$$\beta_{ijk} = \frac{1}{2}\sum_{P}\sum_{e,e'} \frac{\langle g|\mu_r|e\rangle\langle e|\mu_s|e'\rangle\langle e'|\mu_t|g\rangle}{\hbar\omega_e\hbar\omega_{e'}}$$

where $|e\rangle$ and $|e'\rangle$ are excited states, $|g\rangle$ is the ground state, and ω_e and $\omega_{e'}$ are functions of the energy gaps between $|g\rangle$ and $|e\rangle$, $|e'\rangle$. We suggest that the exchange cation can also affect the bond polarizability in a subtly different way. Lowering the electropositivity of the exchange cation will cause a reduction of charge to transfer to the framework and a concomitant decrease in its ionicity as previously stated.[4,23,24] We propose that the energies of these orbitals will be raised by substitution of a more electropositive cation. This effect on the oxygen orbitals may then be expected to be transmitted to the molecular orbitals in which they participate, which will in turn affect the hyperpolarizability through the denominator in the above equation.

(23) Phillips, M. L. F.; Harrison, W. T. A.; Stucky, G. D.; McCarran, E. M.; Calabrese, J., manuscript in preparation.
(24) Phillips, M. L. F.; Harrison, W. T. A.; Gier, T. E.; Stucky, G. D.; Kulkani, G. V.; Burdett, J. K. *Inorg. Chem.* **1990**, *29*, 2158.

The good correlation between Ti(1)–O(9)–Ti(2) angle and SHG intensity is not similarly observed for Ti(1)–O(10)–Ti(2) angle; the latter varying irregularly with cation substitution. We compare the coordination of M(1) and M(2) in the context of the molecular orbital picture described above. The hybridization of the atomic orbitals on O(9) and O(10) can be described as approximately sp^2, with two of the three lobes directed toward the Ti atoms forming σ bonds. The third lobe, along with the remaining p_π orbital, constitute the nonbonding framework electrons available for coordination with M(1) and M(2). We note that the p_π and sp^2 orbitals of O(9) are directed toward M(1) and M(2), respectively, with the converse applying to O(10). If, in the case of O(9), the effect on the NLO coefficient is greater through the sp^2 orbital rather than the p_π orbital, then we should expect substitution at M(1) to have a similar effect through O(10). That this is not observed suggests the possibility of unequal contributions from the two Ti sites to the hyperpolarizability.

It is unclear, however, in what way this argument can explain the nonlinear variation of NLO coefficient with Na content in the KTP–β-NaTP series, since we should expect the same reduction on going from KTP to KNaTP. Although a simple O–M–O moiety may adequately describe the behavior of an isolated MO_6 octahedon, it will need to be expanded in order to incorporate any contributions from extended states.

Conclusion

The effects of cation exchange on the electronic structure of KTP are complex and manyfold, at least with respect to the NLO properties of the material. We can identify one structural feature in the KTP–β-NaTP system that does appear to correlate with the trend in the NLO coefficient: the magnitude of the Ti(1)–O(9)–Ti(2) angle. We know that this trend is also followed by other KTP isomorphs, including NH_4HTP, AgTP, and NaTA.[4,23] We tentatively propose that, on this basis, the main role of the cation may be to modify the degree of delocalisation along the Ti–O chain through its interaction with O(9) and subsequent effect on the Ti(1)–O(9)–Ti(2) angle by way of optimizing its bonding requirements. For example, in the case of Na, this means shorter but not necessarily stronger bonds compared with K. Noting that the value of Ti(1)–O(9)–Ti(2) for KTA is 141.4°,[25] we would predict from the above hypothesis that the NLO response of KTA would be superior to that of KTP, consistent with single-crystal measurements on this material.[26] In contrast, although the value of the Ti–(1)–O(9)–Ti(2) angle for RTP of 137°[27] implies slightly improved NLO performance for this material also, single-crystal SHG data do not show any variation with composition in the system $K_{1-x}Rb_xTiOPO_4$.[18] The significance of determining the structure of the intermediate phase has been the generation of additional structural information without increasing the number of chemical parameters involved. We have been able to evaluate the role of one particular cation in two structures, without the need to account for contributions from other chemical changes.

Acknowledgment. S.J.C. and R.E.M. thank Amoco Technology Co. and the Science and Engineering Research Council respectively for provision of studentships, and R.E.M. also acknowledges funding from Blackwells. We thank Prof. G. D. Stucky for kindly providing a copy of ref 23 prior to publication.

Registry No. $K_{0.42}Na_{0.58}TiOPO_4$, 137540-15-9; $K_{0.43}Na_{0.57}TiOPO_4$, 137540-16-0.

Supplementary Material Available: Observed and calculated structure factors of the ion-exchanged $K_{0.5}Na_{0.5}TiOPO_4$ crystal (29 pages). Ordering information is given on any current masthead page.

(25) Calculated using crystallographic data from: El Brahimi, M.; Durand, J. *Rev. Chim. Mineral* **1986**, *23*, 146.
(26) Bierlein, J. D.; Vanherzeele, H.; Ballman, A. A. *Appl. Phys. Lett.* **1989**, *54*, 783.
(27) Kaduk, J. A.; Jarman, R. H. Unpublished results.